

Discovery of 172-s Pulsations from a Be/X-ray Binary Candidate AX J0051.6–7311 in the SMC with ASCA

Jun YOKOGAWA,¹ Ken’ichi TORII,² Kensuke IMANISHI,¹ and Katsuji KOYAMA^{1*}

¹ Department of Physics, Graduate School of Science, Kyoto University, Sakyo-ku, Kyoto, 606-8502

E-mail(JY): jun@cr.scphys.kyoto-u.ac.jp

² National Space Development Agency of Japan, 2-1-1 Sengen, Tsukuba, Ibaraki, 305-8505

(Received 2000 July 17; accepted 2000 August 8)

Abstract

The results from three ASCA observations of AX J0051.6–7311 = RX J0051.9–7311 are reported. Coherent pulsations with a barycentric period of 172.40 ± 0.03 s were discovered in the third observation, with an exceptionally long exposure time of ~ 177 ks. The X-ray spectrum was found to remain unchanged through these observations, with a photon index of ~ 0.9 . Energy-resolved pulse profiles in the third observation reveal that the pulsations are mostly due to photons with an energy above ~ 2 keV. Archival data of ROSAT and Einstein indicate that AX J0051.6–7311 exhibits a flux variation having a factor $\gtrsim 20$.

Key words: pulsars: individual (AX J0051.6–7311) — stars: emission-line, Be — stars: neutron — X-rays: stars

1. Introduction

Candidates for X-ray binary pulsars (XBPs) in the Small Magellanic Cloud (SMC) have been identified in two ways. Yokogawa et al. (2000a) observed the main body and the eastern wing of the SMC with ASCA, and made systematic analyses on the detected X-ray sources. They found that XBPs and thermal supernova remnants are clearly separated by the spectral hardness ratio. Eight candidates for XBPs were found from this classification. Probably, no detection of coherent pulsations from these candidates is due to the limited photon statistics. On the other hand, Cowley et al. (1997) and Schmidtke et al. (1999) made a systematic search of optical counterparts for X-ray sources. They determined accurate X-ray positions by ROSAT/HRI and made optical photometry and spectroscopy within the X-ray error circles. They identified five X-ray sources with a Be star companion, which are good candidates for XBPs.

The most promising and direct way to establish an XBP is to search for coherent pulsations from these candidates. ASCA observations are suitable for a pulsation search because of high sensitivity in the hard X-ray band. In fact, we searched for coherent pulsations with ASCA from RX J0050.8–7316, a binary with a Be star companion (Cowley et al. 1997), and discovered 323-s pulsations (Imanishi et al. 1999). However, XBPs with a Be star companion are usually in the low-luminosity state of

$\lesssim 10^{36}$ erg s $^{-1}$ (Bildsten et al. 1997; Stella et al. 1986), or a flux of $\lesssim 2 \times 10^{-12}$ erg s $^{-1}$ cm $^{-2}$ at a distance of the SMC (60 kpc is assumed in this paper; van den Bergh 2000). It is difficult to detect coherent pulsations from such a low-flux source for a nominal ASCA exposure time of ~ 40 ks. Therefore, we made an ASCA observation with an exceptionally long exposure time of ~ 177 ks. Within the observed region is located AX J0051.6–7311 = RX J0051.9–7311, which is regarded as an XBP candidate (Yokogawa et al. 2000a), and has also been identified with a Be star companion (Cowley et al. 1997), and is this the most promising target for a pulsation search.

In this letter, we report on the discovery of coherent pulsations from AX J0051.6–7311 (Torii et al. 2000) with a very long exposure observation. We also report a long-term flux history based on investigating the archival data of ROSAT and Einstein.

2. ASCA Observations and Data Reduction

Three ASCA observations (hereafter obs. A1–A3) have covered the position of AX J0051.6–7311. The time spans of these observations were 50765.179–50766.285 (A1), 51309.604–51310.682 (A2), and 51645.986–51651.490 (A3) in units of Modified Julian Day (MJD).

ASCA carries four XRTs (X-ray Telescopes, Serlemitsos et al. 1995) with two GISs (Gas Imaging Spectrometers, Ohashi et al. 1996) and two SISs (Solid-state Imaging Spectrometers, Burke et al. 1994) on each focal plane. In this paper, we do not refer to SIS, because

* CREST, Japan Science and Technology Corporation (JST), 4-1-8 Honmachi, Kawaguchi, Saitama, 332-0012.

AX J0051.6–7311 was outside of the SIS field of view in all observations. The GIS was operated in the normal PH mode in all observations, providing a time resolution of 0.0625 s (high bit rate) or 0.5 s (medium bit rate). We screened the GIS data by rejecting any data obtained in the South Atlantic Anomaly or low cut-off rigidity regions (< 4 GV). Data obtained when the satellite's elevation angle was lower than 5° were also rejected. Particle events were removed by a rise-time discrimination method. After screening, the total available exposure times in obs. A1, A2, and A3 were ~ 43 ks, ~ 41 ks, and ~ 177 ks, respectively. In the following analyses, we use the data from GIS-2 and GIS-3 simultaneously.

3. Results

3.1. Source Identification

In obs. A3, a dim source was detected at $\sim 13'$ from the center of the field of view (FOV). Its position was determined to be $(00^h51^m38^s, -73^{\circ}11'01'')$ with an error of $\sim 1'.5$; thus, we designate it as AX J0051.6–7311. This source was also detected in obs. A1 and A2 at $\sim 21'$ from the center of FOV, with a positional error of $\sim 1'.5$ – $2'$.

In order to determine an X-ray counterpart, we investigated several source catalogs of the Einstein and the ROSAT satellites. An Einstein source No. 25 in Wang and Wu (1992) and a ROSAT source RX J0051.9–7311 (Cowley et al. 1997; Haberl et al. 2000) were found within the error region of ASCA; hence, these would be the same source. Cowley et al. (1997) determined the most accurate position with ROSAT HRI to be $(00^h51^m51^s.4, -73^{\circ}10'38'')$, with a $5''$ error radius. Figure 1 shows a ROSAT HRI image around RX J0051.9–7311 with the error regions of Einstein and ASCA.

3.2. Timing Analyses

In each observation, we collected source photons from a circle centered on AX J0051.6–7311. The radius of the circle was set to be $2'$ in order to avoid contamination from nearby sources located $\gtrsim 4'$ away. After a barycentric correction on the photon arrival times, we performed an FFT (Fast Fourier Transformation) analysis. Only in the power spectrum of obs. A3, we detected an evident peak at a frequency of 0.0058 Hz. The FFT analysis was performed for various energy ranges to maximize the S/N ratio; finally, the maximum power of 59.1 was obtained from the photons in 2.6–8.6 keV (figure 2). The probability to detect such a strong power at any frequency from random events was estimated to be $\sim 8 \times 10^{-8}$, and hence the pulse detection is highly significant. We then performed an epoch folding search, assuming no period change during obs. A3. The barycentric period was determined to be $P = 172.40 \pm 0.03$ s.

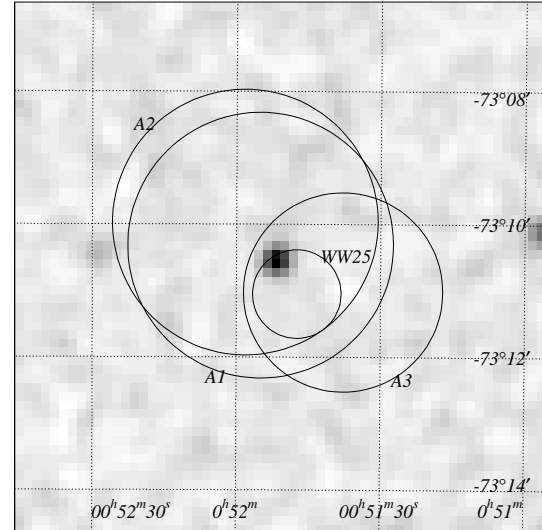


Fig. 1.. ROSAT HRI image (sequence ID. rh600811n00) around RX J0051.9–7311. The error circles of AX J0051.6–7311 (A1–A3) and Einstein source No. 25 (WW25) are overlaid.

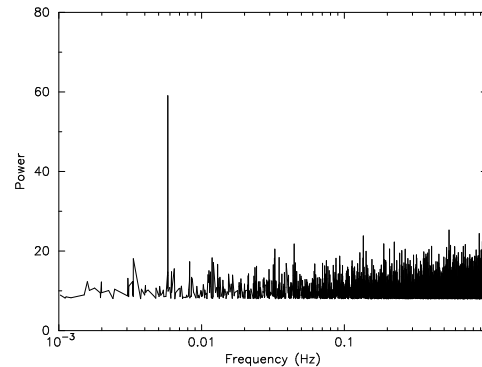


Fig. 2.. Power spectrum in obs. A3. Data points with power less than 8 are omitted. An evident peak is detected at ~ 0.0058 Hz.

Figure 3 shows the pulse profiles in the low- and high-energy bands (0.7–2.6 keV and 2.6–8.6 keV) and their intensity ratio. We clearly found the energy dependence of the pulse profiles; high energy photons are responsible for most of the pulsations. The pulsed fraction, defined as (pulsed flux)/(total flux) without background, is $\sim 60\%$ in 2.6–8.6 keV. To investigate a period change during obs. A3, we divided the observation span in half and performed epoch folding searches on both of the segments; however, no significant period change was detected.

We also examined the aperiodic intensity variation during each observation, by binning the light curves with several time scales from \sim second to \sim hour. Neither a large flux variation nor any burst-like activity was found in each observation. Weak evidence for a random variation of a factor ~ 2 was found in obs. A1 and A3 with a time-scale of 5000–10000 s.

3.3. Spectral Analyses

X-ray spectra were extracted from the same circles used in the timing analyses, while background spectra were from source-free areas near to the source regions.

Figure 4 shows the background-subtracted and phase-averaged spectrum in obs. A3, which has the best statistics. Since no emission line was found in the spectra of obs. A1–A3, we fitted each spectrum to an absorbed power-law model. The spectral parameters (photon index Γ and column density N_{H}) were found to be consistent within the statistical error throughout these observations. Therefore, in order to obtain better statistics, we assumed that Γ and N_{H} are constant in these observations, and simultaneously fitted the three spectra again. We obtained an acceptable fit with the best-fit parameters given in table 1.

For obs. A3, we also extracted phase-resolved spectra from phases 0–0.5 (“on-pulse”) and 0.5–1 (“off-pulse”) (see figure 3). We fitted the spectra to the same model as given in table 1. We found that Γ is much smaller in the on-pulse phase, which is consistent with the energy-resolved pulse shape (figure 3). We also found a hint of soft excess below ~ 1 keV only in the on-pulse spectrum. If we added a blackbody component to the model, the temperature and unabsorbed luminosity were determined to be 0.13 keV and 2×10^{35} erg s $^{-1}$ cm $^{-2}$ (0.7–10.0 keV), respectively, with smaller χ^2 of 35.03 for 27 d.o.f..

4. Discussion

The position of AX J0051.6–7311 has previously been covered by 14 observations of Einstein and ROSAT. We used the archival data of these observations to investigate a long-term flux variation of AX J0051.6–7311. After background subtraction, we derived the count rate of AX J0051.6–7311 in each observation. We then converted the count rate to the flux with the PIMMS software, assuming that Γ and N_{H} are unchanged from the best-fit values for the phase-averaged spectra (table 1). The

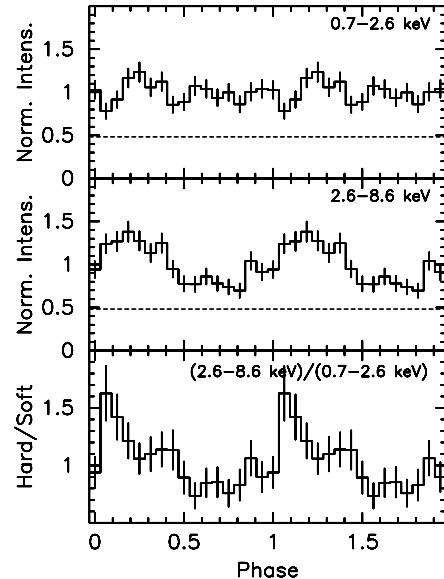


Fig. 3.. Pulse profiles in the 0.7–2.6 keV (upper panel) and 2.6–8.6 keV (middle panel) bands, and the intensity ratio between them (lower panel). Background levels are indicated by broken lines.

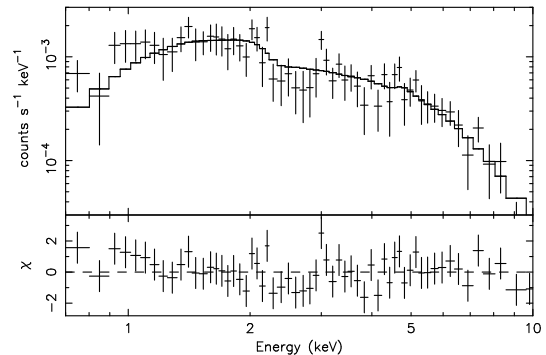


Fig. 4.. Background-subtracted and phase-averaged spectrum from GIS2+3 in obs. A3. Crosses and a solid line indicate data points and the best-fit model, respectively. The best fit model was obtained by the spectral fitting using all the data from obs. A1, A2, and A3, simultaneously.

Table 1. Results of the spectral fitting.

Obs. ID.	Γ	N_{H} (cm $^{-2}$)	Flux (erg s $^{-1}$ cm $^{-2}$)	Luminosity (erg s $^{-1}$)	$\chi^2/\text{d.o.f.}$
— Phase-averaged —					
A1.....	*	*	6.8×10^{-13}	2.9×10^{35}	*
A2.....	*	*	1.5×10^{-12}	6.4×10^{35}	*
A3.....	0.9 (0.8–1.0)	0 ($< 8 \times 10^{20}$)	1.3×10^{-12}	5.6×10^{35}	61.5/69
— Phase-resolved —					
A3: on-pulse.....	0.6 (0.4–0.8)	0 ($< 1 \times 10^{21}$)	1.7×10^{-12}	7.3×10^{35}	43.3/29
A3: off-pulse.....	1.4 (1.1–1.7)	0 ($< 3 \times 10^{21}$)	8.5×10^{-13}	3.7×10^{35}	28.9/24

Note — Parentheses indicate 90% confidence limits. Flux and luminosity are derived from the energy band of 0.7–10.0 keV.

* Γ and N_{H} are linked between the observations.

Table 2. Flux variability of AX J0051.6–7311.

Obs.ID.	Date [*] (MJD)	Instrument	Flux [†] (erg s ⁻¹ cm ⁻²)
E1	43995.264	Einstein/IPC	$< 1.4 \times 10^{-13}$
E2	44189.468	Einstein/IPC	3.4×10^{-13}
E3	44345.640	Einstein/IPC	1.3×10^{-13}
R1	48550.301	ROSAT/PSPC	8.5×10^{-13}
R2	48732.665	ROSAT/PSPC	7.7×10^{-13}
R3	48963.036	ROSAT/PSPC	$< 3.8 \times 10^{-14}$
R4	49093.121	ROSAT/PSPC	$< 8.6 \times 10^{-14}$
R5	49118.070	ROSAT/PSPC	3.4×10^{-13}
R6	49298.538	ROSAT/PSPC	3.4×10^{-13}
R7	49321.271	ROSAT/PSPC	6.7×10^{-13}
R8	49652.016	ROSAT/HRI	8.9×10^{-13}
R9	49864.713	ROSAT/HRI	1.2×10^{-12}
R10 ...	50055.454	ROSAT/HRI	1.8×10^{-12}
R11 ...	50412.933	ROSAT/HRI	6.5×10^{-13}
A1	50765.732	ASCA/GIS	6.8×10^{-13}
A2	51310.143	ASCA/GIS	1.5×10^{-12}
A3	51648.738	ASCA/GIS	1.3×10^{-12}

* Middle of the observations.

† In the 0.7–10.0 keV band.

results are given in table 2. We found that AX J0051.6–7311 may have been brightest in the ASCA observations. The largest flux difference having a factor $\gtrsim 50$ is found between obs. R3 and obs. R10, although there may be some systematic error between different instruments (PSPC and HRI). However, even if we restrict the flux comparison within the same instruments, we find a flux difference having a factor $\gtrsim 20$ between obs. R1 and obs. R3 (PSPC). Such a large flux variation, together with the long period (172 s), hard spectrum ($\Gamma = 0.9$), and a Be star counterpart, suggests that AX J0051.6–7311 should be an XBP with a Be star companion.

A small bump is found in the pulse profile of the lower energy band (figure 3; phase 0.1–0.4). The soft excess detected in the on-pulse phase implies existence of a pulsating soft component found in some XBPs (e.g., Her X-1, Endo et al. 2000; LMC X-4, Woo et al. 1996; XTE J0111.2–7317, Yokogawa et al. 2000b), although better statistics are necessary to lead to a rigid conclusion; a simple power-law model is also accepted for the on-pulse spectrum within 95% confidence level (see table 1).

Coherent pulsations were detected only from the data of obs. A3. We suggest that this is simply due to the much improved statistics in obs. A3, with the unusually long exposure time (~ 177 ks). Indeed, when we divided obs. A3 into four segments, each having an exposure time of ~ 40 ks, we could not detect significant coherent pulsations from any of these segments neither by the FFT analysis nor by the epoch folding search. We also could not detect coherent pulsations from obs. R2, which has the best statistics among the ROSAT/Einstein observa-

tions. Coherent pulsations have been detected from all of the hard X-ray sources in the SMC with a luminosity of $\gtrsim 10^{36}$ erg s⁻¹ cm⁻² (Yokogawa et al. 2000a), within a typical ASCA exposure of ~ 40 ks. Pulsations from fainter hard X-ray sources, AX J0051.6–7311 and 1SAX J0103.2–7209, with luminosities of $\sim 5 \times 10^{35}$ erg s⁻¹ cm⁻², were also detected with much longer exposures (this work and Yokogawa et al. 2000a). These facts strongly suggest that a significant fraction of the unidentified hard sources in Yokogawa et al. (2000a) with a luminosity of $\lesssim 10^{36}$ erg s⁻¹ cm⁻² are XBPs. Therefore, a long observation like obs. A3 is highly required to extend the pulsar population study to the low luminosity side.

The Einstein and ROSAT data were obtained through the High Energy Astrophysics Science Archive Research Center Online Service, provided by the NASA/Goddard Space Flight Center. J.Y. is supported by JSPS Research Fellowship for Young Scientists.

References

Bildsten L., Chakrabarty D., Chiu J., Finger M.H., Koh D.T., Nelson R.W., Prince T.A., Rubin B.C. et al. 1997, ApJS 113, 367

Burke B.E., Mountain R.W., Daniels P.J., Dolat V.S., Cooper M.J. 1994, IEEE Trans. Nucl. Sci. 41, 375

Cowley A.P., Schmidtke P.C., McGrath T.K., Ponder A.L., Fertig M.R., Hutchings J.B., Crampton D. 1997, PASP 109, 21

Endo T., Nagase F., Mihara T. 2000, PASJ 52, 223

Haberl F., Filipović M.D., Pietsch W., Kahabka P. 2000, A&AS 142, 41

Imanishi K., Yokogawa J., Tsujimoto M., Koyama K. 1999, PASJ 51, L15

Ohashi T., Ebisawa K., Fukazawa Y., Hiyoshi K., Horii M., Ikebe Y., Ikeda H., Inoue H. et al. 1996, PASJ 48, 157

Schmidtke P.C., Cowley A.P., Crane J.D., Taylor V.A., McGrath T.K., Hutchings J.B., Crampton D. 1999, AJ 117, 927

Serlemitsos P.J., Jalota L., Soong Y., Kunieda H., Tawara Y., Tsusaka Y., Suzuki H., Sakima Y. et al. 1995, PASJ 47, 105

Stella L., White N.E., Rosner R. 1986, ApJ 308, 669

Torii, K., Yokogawa, J., Imanishi, K., Koyama, K. 2000, IAU Circ. 7428

van den Bergh S. 2000, PASP 112, 529

Wang Q., Wu X. 1992, ApJS 78, 391

Woo J.W., Clark G.W., Levine A.M., Corbet R.H.D., Nagase F. 1996, ApJ 467, 811

Yokogawa J., Imanishi K., Tsujimoto M., Nishiuchi M., Koyama K., Nagase F., Corbet R.H.D. 2000a, ApJS in press

Yokogawa J., Paul B., Ozaki M., Nagase F., Chakrabarty D., Takeshima T. 2000b, ApJ 539, 191